# Cross-bispectral analysis of the electromagnetic field in a beam-plasma interaction

Laurence Rezeau, G. Belmont, B. Guéret, Bertrand Lembège

JOURNAL OF GEOPHYSICAL RESEARCH, VOL. 102, NO. A11, PAGES 24,387–24,392, NOVEMBER 1, 1997

# Cross-bispectral analysis of the electromagnetic field in a beam-plasma interaction

L. Rezeau, G. Belmont, B. Guéret and B. Lembège

Centre d'Etude des Environnements Terrestre et Planétaires, Vélizy, France

**Abstract.** The use of bicoherence has proved its efficiency in the analysis of nonlinear wave interactions. The method has been adapted to interpret the results of a simulation of the beam-plasma interaction, in a case of broadband spectra, where many unstable modes can be suspected to couple. As the interacting waves exhibit different polarizations (electrostatic and electromagnetic), the bicoherence has been modified into a cross bicoherence in order to test the coupling of different field components. The visualization of the result has been designed in order to evidence the couplings in terms of efficiency (high bicoherence) and energy (high power). The application of this method to the simulation results shows that quadratic wave interactions are effective; new helpful information is stressed in order to interpret the observed growth of large-scale magnetic fluctuations.

## 1. Introduction

Bicoherence is the appropriate tool for analyzing quadratic couplings [Kim and Powers, 1979]. This tool is developed here in order to analyze numerical results obtained from a particle-in-cell simulation of a beam-plasma interaction; the main difficulties to be solved in this case are (1) the buildup of a broadband spectrum of the fields and (2) the vectorial nature of the problem, i.e., the large number of different electromagnetic components that may couple nonlinearly. The solutions developed for this analysis should obviously be applicable in any data set, from experiment or from other numerical simulations, where these difficulties are met, which is not a rare occurrence. Generally speaking, when waves are observed to grow, one is led to the following tests: (1) Does linear theory apply? (2) If not, do the nonlinear physical effects consist of weak or strong interactions? In the case of a linear situation, the appropriate analysis tool is the Fourier analysis. In the case of weakly nonlinear interactions, higher-order spectral analysis is needed: bispectral analysis for quadratic coupling, trispectral analysis for cubic coupling, etc. [*Lefeuvre et al.*, 1995]. In the case of strong turbulence, all spectral tools fail, and other data processing must be performed [*Dudok de Wit*, 1996]. In the present analysis we will limit the investigation to third-order spectral analysis (bispectrum and bicoherence), since it is conclusive we have not tested higher-order analysis.

The bispectral analysis has proved its efficiency for analyzing three-wave couplings, from a theoretical point of view [*Kim and Powers*, 1979] and in experiments [*Grésillon and Mohamed-Benkadda*, 1988]. When two Fourier components $k_1$ and $k_2$ of a given signal $s(k)$ couple and give rise to a third wave number $k_3 = k_1 + k_2$, the bispectrum is maximum at the point $(k_1, k_2)$ of the two-dimensional wave number space. At this point, the bicoherence tends toward 1. Most of the published tests of this method have been performed in cases where the three-wave coupling could be guessed in advance, either because of the experimental conditions [*Lefeuvre et al.*, 1995] or because the spectrum of the signal was simple enough to make a visual inspection efficient (three quasi-monochromatic waves respecting $k_3 = k_1 + k_2$ [*Kim and Powers*, 1979]). In the present study, we will show that this analysis can be used also as a means of exploring a physical situation where the interpretation cannot be known prior to the analysis.

The physical problem which is studied here is a beam-plasma interaction studied with the help of a full particle numerical simulation. The geometry of the problem is one-dimensional in space, but all field vectors have three components, which allows a fully electromagnetic interaction between the beam and the plasma. As expected in such an interaction, electrostatic waves are unstable [see, for instance, *Akhieser et al.*, 1967; *Cap*, 1978; *Delcroix and Bers*, 1994]. What is going to be investigated here is the nature of the source mechanism of the electromagnetic waves which are observed shortly after the growth of the electrostatic modes.

After giving the definitions commonly used for bispectrum and bicoherence and the type of visualization adopted, the application of the method to the beam-plasma problem will be described, and we will show how the results can be interpreted theoretically in terms of nonlinear wave couplings.

## 2. Bispectrum and Bicoherence: Tools for Wave Coupling Analysis

### 2.1. Definitions

The bispectrum and bicoherence are defined after Fourier transform of the data. The simulation box is considered at a given time, and the Fourier transform is performed in space, giving Fourier components $X_l$, $Y_m$, and $Z_{l+m}$, for three different physical components of the electromagnetic field, functions of a one-dimensional wave number $k$ ($X_l = X(k_l)$).

The standard definition of the bispectrum is $B(k_l, k_m) = \langle X_l X_m X^*_{l+m} \rangle$ [*Kim and Powers*, 1979; *Kravtchenko-Berejnoi et al.*, 1995], where angle brackets denote an average (to be defined below). This definition will



Paper number 97JA01994.
0148-0227/97/97JA-01994$09.00

be replaced here by a cross bispectrum $B(k_l,k_m)=\langle X_l Y_m Z^*_{l+m}\rangle$. This definition does not change the mathematical treatment of the bispectrum or bicoherence, but it allows testing mode coupling more efficiently if the interacting modes have different polarizations, for instance electrostatic and electromagnetic. It also can be useful whenever a theoretical hypothesis can be made about the nature of the coupling terms: One should take, for instance, $X = j_x$, $Y = B_y$ and $Z = v_z$ if a nonlinear term **jxB** is suspected to produce changes in a $m\partial_t(v)$ term (where $\partial_t$ stands for the partial derivative with respect to the time $t$).

The bicoherence is the normalized square modulus of bispectrum. Different kinds of normalization are possible [Kravtchenko-Berejnoi et al., 1995] ; the normalization which is used here is

$$b(k_l,k_m)=\frac{|\langle X_l Y_m Z^*_{l+m}\rangle|^2}{\langle|X_l Y_m Z^*_{l+m}|\rangle^2}$$

It is the less sensitive to possible nonstationarity of the signal, and it gives a symmetrical role to the different components, which is the most satisfactory in the case they are all different.

### 2.2. Estimation

In the theoretical definition of the bispectrum or bicoherence, the average (angle brackets) is an ensemble average, calculated over successive independent realizations of a given experiment [*Grésillon and Mohamed-Benkadda*, 1988]. When the signal is known over a long time series (or spatial series, in our case), an ergodicity hypothesis can be applied: The original interval is divided into N subintervals, and the estimate of <*f*> is

$$1/N\sum_{i=1}^{N} f_i$$

The number of subintervals is chosen with the following compromise: The error on the bispectrum estimate is proportional to 1/N which makes the highest value of N the best; on the other hand, the resolution $\Delta k$ of the spatial spectrum is proportional to N, and it must be small enough to separate the different modes that couple in the problem. In the present case, the length of the simulation box is $L = 2048\ \Delta x$ (where $\Delta x$ is the grid step); it has been divided it into eight smaller boxes of 256 points.

### 2.3. Visualization

The definitions of bispectrum and bicoherence given above show that two kinds of information can be obtained. The bicoherence gives only the phase coherence of the signals with no information about the energy contained in them, so that a high bicoherence may be due to weak components which are a minor part of the total signal. This leads to an unpleasant drawback: As the number $N$ of samples used is not infinite ($N = 8$ in our case), the statistical validity of the result is thus limited, and increasing the number of weak components acting on the result would obviously increase the number of coincidental high values of the bicoherence. On the other hand, the bispectrum contains the same information about the phases but multiplied by the amplitudes of the three components, and a weak coherence can be counterbalanced by a high intensity. The relevant information of interest herein is doublets ($k_l$, $k_m$), where both the bicoherence and the bispectrum are high, which means that the mode coupling exists and is energetically efficient, and consequently where a significant energy transfer can take place. To find the modes where this coupling exists, it would be necessary to plot both quantities. Instead of that, we plot the bispectrum filtered by the bicoherence; that is, the bispectrum is plotted in color code only when the bicoherence exceeds a given threshold.

## 3. Wave Generation by Beam-Plasma Interaction

### 3.1. The Simulation

The beam-plasma interaction is simulated with a one-dimensional fully electromagnetic particle code [*Krafft et al.*, 1994] in which ions are at rest (they form a neutralizing background); the vectors ($v$, $E$, $B$) are three dimensional. The simulation box is 2048 points long, with periodic boundary conditions. Initially, the ratio of electron gyrofrequency over plasma frequency is equal to 0.079, the

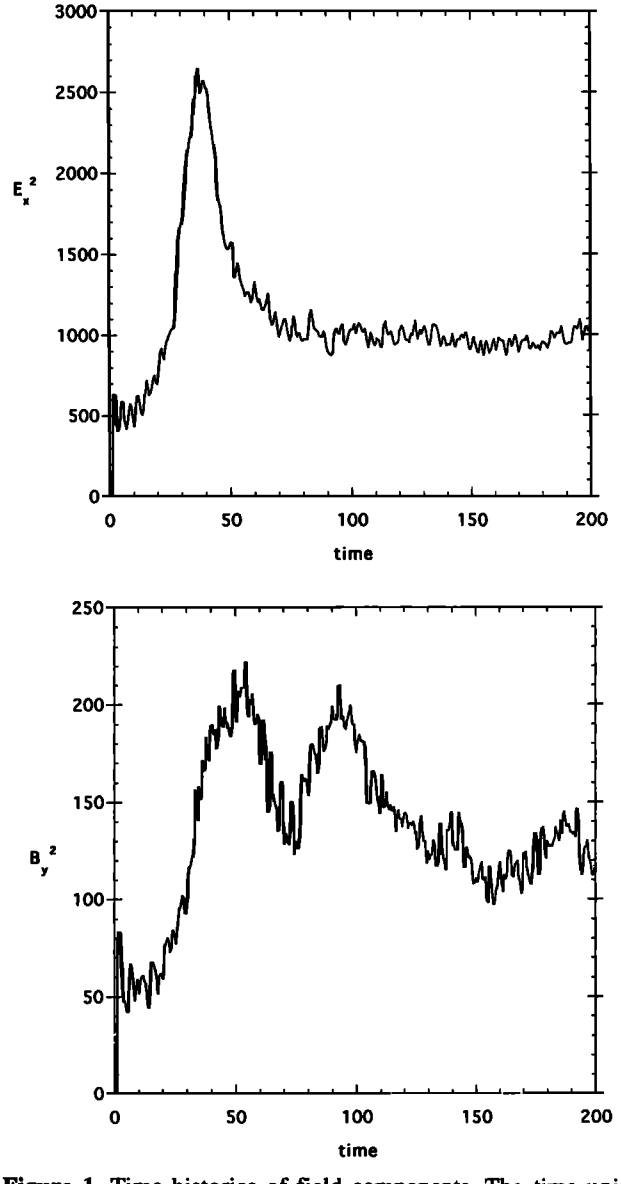


**Figure 1.** Time histories of field components. The time unit is $\omega_{pe}^{-2}$, and the E and B fields are normalized so that the energies are comparable (the electric field is divided by $E_0 = (m/q)\Delta x\omega_{pe}^2$, where $\Delta x$ is the grid step, and the magnetic field is devided by $E_0/c$).

beam density is 12% of the plasma density, the velocity of the beam is 3.5 times the plasma thermal velocity, and the thermal velocity of the beam is 0.3 times the plasma thermal velocity. The angle between the magnetic field and the wave propagation direction is 31°. The $x$ direction is the direction of the simulation box and of the wave propagation; $B_x$ is equal to 0, $E_x$ is the electrostatic component of the field, and the $y$ and $z$ components are the electromagnetic components (the $z$ axis is chosen in such a way that the static magnetic field is in the $(x, z)$ plane. Figure 1 shows the energy time histories for two components (one electrostatic and one electromagnetic). As expected, there isa large increase of the electrostatic energy until $t = 40$ (in the simulation time unit, which is equal to $\omega_{pe}^{-1}$). Moreover, one observes that shortly after the increase of electrostatic energy, the electromagnetic energy increases too, and this unusual feature is at the origin of this study.

### 3.2. Simulation Results Against Linear Interpretation

Let us first determine which of the simulation results are in agreement with the linear properties of the system and therefore which results need weak or strong nonlinear effects to be interpreted. As the classical beam-plasma instability is purely electrostatic, it is interesting, in particular, to check whether the magnetic components observed must be attributed to unusual linear properties (due to the existence of a static magnetic field at an oblique angle from the propagation direction) or if they are a consequence of nonlinear effects. The calculation of the linear properties has been done using the program WHAMP (Waves in Homogeneous, Anisotropic, Multicomponents Plasmas) which solves the kinetic dispersion relation of plane waves in a hot magnetized plasma [*Rönnmark*, 1982]. The WHAMP input parameters have been determined to fit the initial conditions of the simulation, and the main results are summarized as follows :

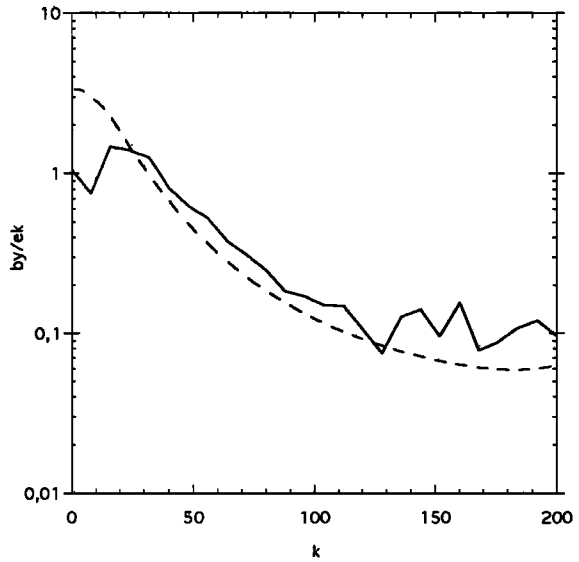


**Figure 2.** The ratio $B_y/E_x$ in simulation units (the magnetic field is multiplied by the light velocity). A ratio equal to 1 represents electromagnetic waves with equal energy on the magnetic and on the electric components. The simulation results are plotted as a solid line, and the WHAMP results are plotted as a dashed line.

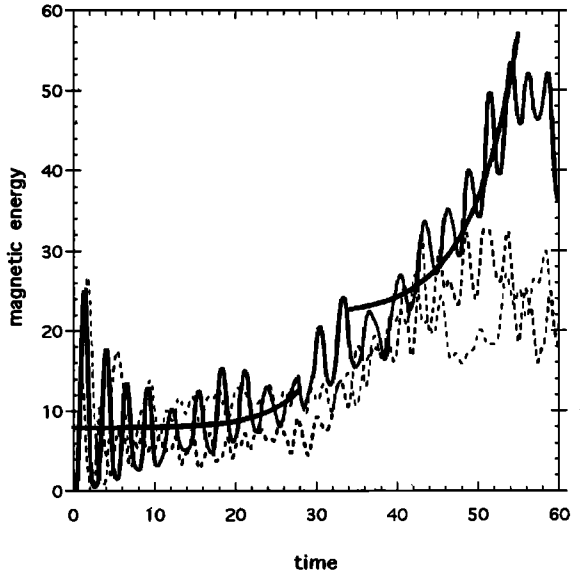


**Figure 3.** Magnetic energies $B_y^2$ for three mode ranges: (25, 35), (35, 45), and (45, 55). The intermediate range ($35 < k < 45$, shown by the thin solid line) is observed to get higher values than the two adjacent ranges (dashed lines) from the time $t \approx 40$. The superimposed bold lines are fits with exponential functions corresponding to growth rates computed with the program WHAMP (from the initial beam conditions for $t < 30$ and from the modified beam measured in the simulation for $t > 40$) and adjusted for estimated quasi-linear effects.

1. Apart from the "light waves," all of the observed modes, electrostatic as well as electromagnetic, belong to the same branch of the dispersion relation, generally referred to as "beam mode." This mode appears mainly electrostatic close to the maximum growth rate wavenumber ($k \approx 110$) but gets a nonnegligible $B_y$ component for smaller wavenumbers ($k < 70$). This result is illustrated in Figure 2, where both ratios $B_y/E_x$ are plotted versus the wavenumber, from the simulation results and from the linear calculation of the beam mode. It can be observed that the agreement is quite good, except for the smaller values of the wave number, where the waves propagating on the beam mode have amplitudes which are smaller than the coexisting light-mode waves so that the calculated ratios are no more comparable.

2. Interpreting the amplitudes reached by the $B_y$ component with only the knowledge of the linear properties is a more tricky problem. Two difficulties occur: (1) The quasi-linear wave-particle interactions make the instantaneous growth rate decrease with time during the overall growth of the electric energy, ultimately leading to the wave saturation, and (2) the level reached at a given time during the growth period depends *a priori* not only on the growth rate but also on an unknown "initial" condition. As the large amplitude magnetic component is observed noticeably after the electrostatic maximum ($t \approx 40$), this growth, even when it can be correctly fitted by a linear or quasi-linear growth for times $40 < t < 60$, is likely to have been initialized at $t \approx 40$ by nonlinear couplings with electrostatic waves. This second hypothesis seems to be confirmed by Figure 3, where the magnetic energy $B_y^2$ is displayed as a function of time for three successive mode ranges: $25 < k < 35$, $35 < k < 45$, and $45 < k < 55$.

The central mode band (bold line) can be observed to get an impetus between 30 and 40 and to grow afterward to higher values than the two adjacent bands. The superimposed bold lines on Figure 3 show that the numerical results can be fitted with exponential functions (with growth rates calculated thanks to the WHAMP program and adjusted for quasi-linear effects) under the condition that the initial value is chosen larger for $40 < t < 50$ than for $0 < t < 30$. If this guess is correct, mode couplings should exist at $t \approx 40$ and for $k$ in the range $35 < k < 45$; however, as these couplings are observed to respect most of the linear properties, they are likely to be weak nonlinear effects, so that the bispectrum analysis should allow to confirm or invalidate their existence. Let us finally notice that the whistler mode, which could have been envisaged a priori for interpreting the magnetic growth, concerns indeed much lower frequencies and that its growth rate is 1 order of magnitude smaller. It can clearly be ruled out.

### 3.3. Bicoherence Analysis

The bispectrum filtered by the bicoherence is displayed on Figure 4 at time $t = 40$. The components which are correlated are $E_x$, $E_x$ and $B_y$ (the combination of $E_x$, $B_y$ and $B_y$ has been tested also, as well as other combinations, and happens to give no result, which is not surprizing since the primary instability is electrostatic), with respective wave numbers $k_1$ (horizontal axis), $k_2$ (vertical axis) and $k_1 + k_2$ for the third component. All the shaded squares are the regions of the $(k_1, k_2)$ plane where the bicoherence is higher than 0.75. The grey scale inside these regions indicates the value of the bispectrum. It shows that for many couples $(k_1, k_2)$ the bicoherence is high, with a low energy contained in the modes ($k_1$ and $k_2 > 150$); these wave couplings, if real, are not efficient, and they are likely to be accidental. In contrast, around $k_1 = 140$, the wave coupling is efficient with $k_2$ between -50 and -100. The result is therefore an electromagnetic mode with $k_3$ between 40 and 90. As two of the three components are identical ($E_x$), there is a redundancy in the plot: An electrostatic mode with $-100 < k_1 < -50$ couples as well with a mode at $k_2 = 140$, to produce an electromagnetic component at $40 < k_3 = k_1 + k_2 < 90$. This explains the symmetry of the figure with respect to the diagonal. An important point should be underlined at this stage: The bispectral analysis evidences a coupling between three wavenumbers but does not give any information about the direction of the energy transfer. Does the coupling work in the direction described above, or does an electrostatic component couple with an electromagnetic one to produce the other electrostatic component? The answer is not given by this analysis, but the simple visual inspection of the spectrograms (Figure 5) of the components is sufficient here to conclude that the first solution is the right one. These plots show that the $B_y$ component appears when the electrostatic modes are yet at their maximum. Then, the electromagnetic modes are likely to be created by the electrostatic ones and not the opposite.

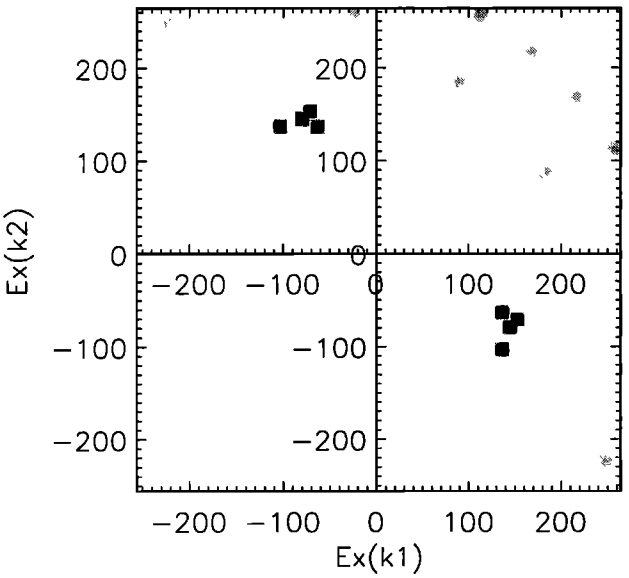


**Figure 4.** Bispectrum filtered by bicoherence at time $t = 40$. The horizontal axis is the wave number of the $E_x(k_1)$ component, and the vertical axis is the wave number of the $E_x(k_2)$ component. The third component is $B_y(k_1 + k_2)$. The grey scale goes from white for low energies to black for the highest ones. See text for more detail.

## 4. Interpretation

The linear analysis has shown that most of the observed properties (dispersion and polarization) are those of the so-called "beam mode." The only possible disagreement with the linear properties concerns the energy wave growths: Energy transfers seem to occur from the most unstable part of the mode (electrostatic) toward the smaller wave number part (electromagnetic). The bispectral analysis has evidenced phase correlation between $E_x$, $E_x$, and $B_y$, characteristic of quadratic couplings between these three components. The existence of the weak nonlinear effects which could be anticipated from the linear analysis has thus been confirmed. As the possibility of creating a magnetic component from the coupling of two electrostatic ones may seem paradoxical, let us identify the quadratic terms in the equations that can be responsible for this phenomenon and try to provide a heuristic interpretation.

Searching for the quadratic terms able to excite the large-scale mode (implying $B_y$), it is sufficient to focus on the momentum transport equation of the beam electrons:

$$\partial_t(n_b m v_{bz}) + \partial_x(n_b m v_{bx} v_{bz} + p_{bxz}) = -n_b e\left[E_z + v_{bx} B_y - v_{by} B_x\right]$$

where $p_{bxz}$ is the $x$-$z$ component of the electron beam pressure tensor.

We have selected here the $z$ component of the vectorial equation: on the beam mode, the perturbation of the beam electron velocity $v_b$ is mainly in the $x$-$z$ plane; the $x$ component corresponds to the electrostatic component of the phenomenon (predominant close to the maximum growth rate), while the $z$ component, which exists only for oblique propagation, is associated with the magnetic field perturbation $B_y$ via the $j_z$ current (predominant for small wave numbers). Looking at the $v_{bz}$ component, we shall therefore focus on the most interesting electromagnetic side of the quadratic coupling.

Each of the two electrostatic modes which are supposed to couple are essentially characterized by their perturbations of the beam electron density $n_{b1}^1$ and $n_{b2}^1$ and the corresponding perturbations of the $x$ velocity $v_{bx1}^1$ and $v_{bx2}^1$; the magnetic

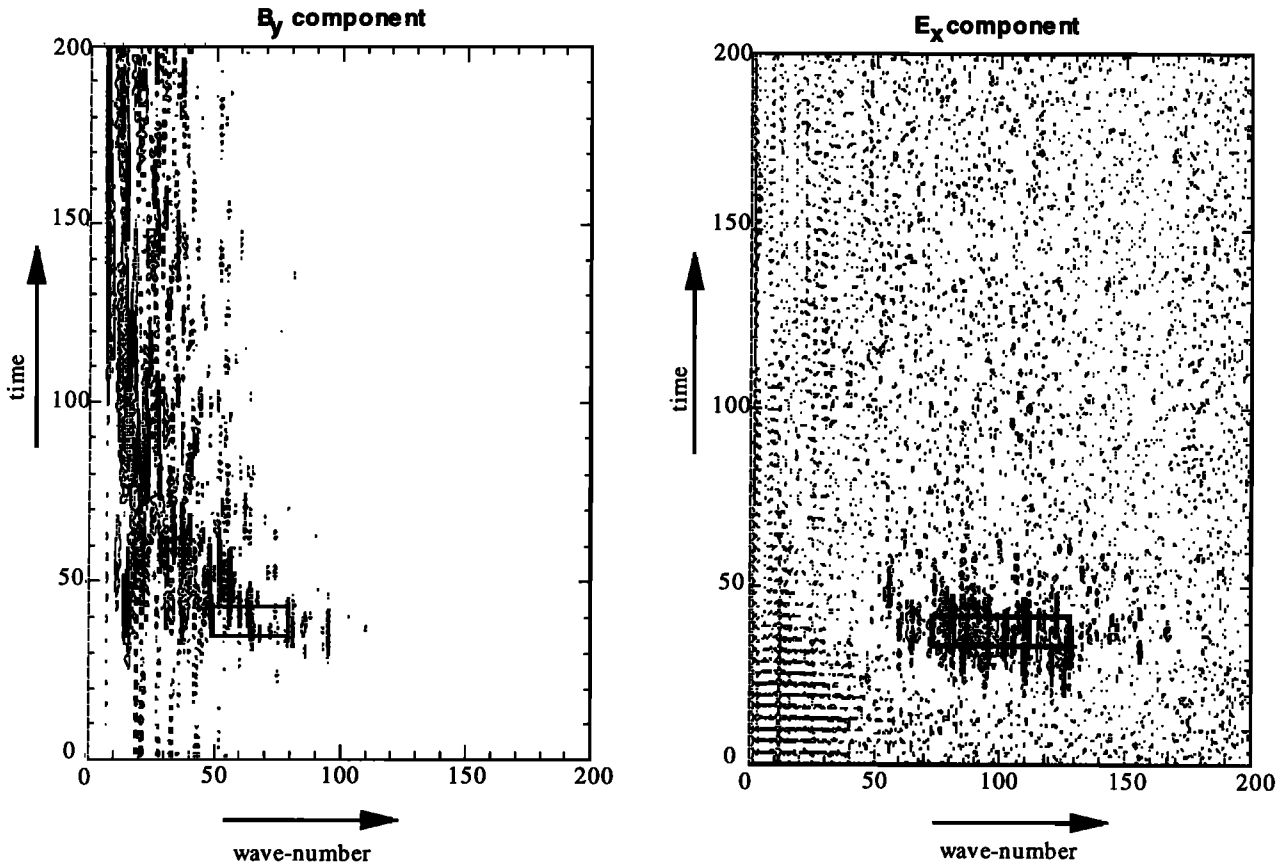


**Figure 5.** Spectrograms of the field components. The horizontal axis is wavenumber, and the vertical axis is time. The rectangles show the mode ranges which are shown to couple in Figure 4.

perturbation $B_y^1$ is negligible as well as is the $E_z^1$ perturbation. In these conditions, the only quadratic term able to excite the electromagnetic mode (involving $v_{bz}^1$ and $B_y^1$) from these two electrostatic modes is

$$\partial_x(n_b^1 m v_{bx}^1)v_{bz0}$$

It then becomes apparent that the electromagnetic mode corresponds to a linear momentum perturbation $n_{b0}mv_{bz}^1$ of the beam electrons excited by a nonlinear flux of momentum $n_b^1 m v_{bx}^1 b_{bz0}$, where the density perturbation $n_b^1$ is due to one electrostatic perturbation, the velocity perturbation $v_{bx}^1$ to a second electrostatic perturbation, and the transport velocity $v_{bz0}$ is due to the $z$ component of the zero-order velocity of the beam (null for parallel propagation).

The possibility of generating electromagnetic waves from the coupling of electrostatic ones is however not entirely new. This possibility has been suggested in particular in *Lavergnat et al.* [1982] in the frame of the French-Soviet ARAKS (Artificial Radiation and Aurora between Kerguelen and the Soviet Union) experiment for explaining the emission of electromagnetic waves from a cylindrical electron beam injected in the ionosphere. As in the present interpretation, it was shown that the modulation of the electron beam due to the beam-plasma instability is responsible for the electromagnetic emission; the physical mechanisms involved in this case were of the same nature as those concerning the emissions from other beam inhomogeneities: wave front [*Lavergnat and Pellat*, 1979] or beam artificially modulated [*Krafft et al.*, 1994, and references therein]. One of the main differences with the present work is that the electromagnetic waves were propagating on the whistler mode for all these studies (allowing to radiate outside the electron beam in the ARAKS experiment) and not on the beam mode as in the present study.

## 5. Conclusion

The bispectrum is an appropriate tool for evidencing quadratic wave coupling as in the present study of beam-plasma interaction. It is especially interesting when the fluctuations that are investigated have a wideband spectrum so that a visual inspection of the spectrum cannot give information about the coupling. The use of cross bispectrum is necessary when one considers electromagnetic fields because of the different polarizations involved: The electromagnetic mode, for instance, which is clearly visible on the transverse magnetic component $B_y$, is much more difficult to detect on the $E_x$ component where it is negligible, and conversely, the quasi-electrostatic modes cannot be detected on the magnetic data. Bispectrum and bicoherence contain two different types of information, which are both necessary to evidence efficient wave coupling. The combined visualization used here is a compromise that allows to grasp the two aspects in one plot. This method can be applied to any one-dimensional series, function of space (as done in this paper), or time, to evidence coupling in wavenumber or in frequency.

Nevertheless, in the present study, a limitation of the method appears when one considers the temporal evolution of the phenomena. We have performed here a spectral analysis at a given time, in the wavenumber space. The analysis of the dispersion relations of all the modes that can propagate in such a situation shows that for one value of the wavenumber, different frequencies can exist, and a more comprehensive approach would consist of considering a two-dimensional spectral analysis, with time and space Fourier transforms. This method needs two-dimensional series to evidence coupling in the ($\omega$, k) space (or in ($k_x$, $k_y$) space) and therefore needs much more computer time. It is still under development, and it is already needed for numerical simulation data processing and will also be useful for multispacecraft missions data.

Acknowledgments. The authors thank F. Lefeuvre and H. de Féraudy for fruitful discussions.

The Editor thanks F. Lefeuvre and K. Rönnmark for their assistance in evaluating this paper.

## References

Akhieser, A. I., I. A. Akhieser, R. V. Polovin, A. G. Sitenko, and K. N. Stepanov, *Collective Oscillations in a Plasma*, Pergamon, Tarrytown, N.Y.,1967.

Cap, F., *Handbook on Plasma Instabilities*, vol. 2, Academic, San Diego, Calif., 1978.

Delcroix, J. L. and A. Bers, *Physique des Plasmas*, vol. 2, InterEditions / CNRS Editions, Paris, France, 1994.

Dudok de Wit, T., Analysis techniques for resolving nonlinear processes in plasmas, in *Review of radio Science*, edited by W. Ross Stone, pp. 781-806,Oxford University Press, Oxford, Great Britain, 1996.

Grésillon, D., and M. S. Mohamed-Benkadda, Direct mode-mode coupling observation in the fluctuations of non-stationary transparent fluid, *Phys. Fluids, 31*(7), 1904-1909, 1988.

Kim, Y. C., and E. J. Powers, Digital bispectral analysis and its application to nonlinear wave interactions, *IEEE Trans. Plasma Sci., PS 7*, 120-131, 1979.

Krafft, C., G. Matthieussent, and B. Lembège, Numerical simulation of Cerenkov whistler emission by a modulated beam, *Phys. Plasma, 1*(12), 1-7, 1994.

Kravtchenko-Berejnoi, V., V. Krasnosselskikh, D. Mourenas, and F. Lefeuvre, Higher-order spectra and analysis of a nonlinear dynamic model, in *Proceedings of the CLUSTER Workshop on Data Analysis Tools at Braunschweig, Deutschland, ESA SP-371*, pp. 61-67, ESA, Noordwijk, The Netherlands,1995.

Lavergnat, J., and R. Pellat, High-frequency spontaneous emission of an electron beam injected into the ionospheric plasma, *J. Geophys. Res., 84*, 7223-7238, 1979.

Lavergnat, J., D. Le Queau, R. Pellat, and A. Roux, Nonlinear radiation by an electron beam in the whistler range: A tentative theoretical model, *Phys. Fluids, 25*(6), 1073-1082, 1982.

Lefeuvre, F., V. Kravtchenko-Berejnoi, and D. Lagoutte, Introduction to the analysis of Bi-linear and Tri-linear processes in Space plasmas, in *Proceedings of the CLUSTER workshop on data analysis tools at Braunschweig, Deutschland, ESA SP-371*, pp. 51-59, ESA, Noordwijk, The Netherlands,1995.

Rönnmark, K., WHAMP-Waves in homogeneous, anisotropic, multicomponents plasmas, *Rep. 179*, Kiruna Geophys. Inst., Kiruna, Sweden, 1982.

G. Belmont, B. Guéret, B. Lembège, and L. Rezeau, Centre d'Etude des Environnements Terrestre et Planétaires - UVSQ/CNRS, 10/12 avenue de l'Europe, F-78140 Vélizy, France. (e-mail: rezeau@cetp.ipsl.fr)

(Received April 8, 1997; revised June 24, 1997;
accepted July 1, 1997.)